J Appl Electrochem (2008) 38:1659–1664
DOI 10.1007/s10800-008-9613-4

ORIGINAL PAPER

A novel nanocomposite of Pd nanocluster/poly(*N*-acetylaniline) nanorod modified electrode for the electrocatalytic reduction of oxygen

Chumming Jiang · Xiangqin Lin

Received: 14 November 2007 / Accepted: 27 May 2008 / Published online: 10 June 2008

Abstract A novel nanocomposite of palladium nanoclusters/poly(*N*-acetylaniline) nanorods was electrodeposited on to a glassy carbon electrode by cyclic voltammetry (CV). This electrode, Pd/PAANI/GCE, was characterized by X-ray photoelectron spectroscopy (XPS), field emission scanning electron microscopy (FE-SEM), X-ray diffraction (XRD), CV and chromoamperometry. It was demonstrated that the ball-shaped Pd nanoclusters were mainly growing on the ends of the nanorods, forming a novel nanocomposite. The preliminary study also demonstrated that the electrode modified with this nanocomposite matrix had high electrocatalytic activity toward 4-e^- oxygen reduction.

Keywords Nanocomposite · Poly(*N*-acetylaniline) · Palladium nanocluster · Oxygen reduction · Electrocatalysis

1 Introduction

Electrochemical reduction of oxygen has been the subject of extensive studies in view of its importance in the detection of oxygen levels for fish culture, biochemistry, neuroscience and physiology [1–7]. It is especially important for realization of highly efficient fuel cells, batteries and other electrode applications. Many different electrode materials have been utilized as efficient electrocatalysts towards the oxygen reduction reaction (ORR). Several metal nanoparticles and metal-based alloys have been used for fabrication of modified electrodes for this purpose [1, 8–13]. In addition, the dispersion of metal particles on to a matrix has been demonstrated to be a convenient way to reduce the particle size for enhanced electrocatalytic activity. The matrix of carbon nanotubes (CNTs) adsorbed on to the electrode surface has advantages for the electrodeposition of metal nanoparticles for electrocatalytic ORR [14–18].

Besides CNTs, organic conducting polymers can also be exploited as conducting matrices and provide large surface area for the deposition of particulate catalysts. The most commonly studied conducting polymers such as polyaniline, polypyrrole and polythiophene have been investigated as conductive matrices for electrocatalysis of the reduction of protons and oxygen [19–23] and the oxidation of small organic molecules such as methanol and formic acid [24–26].

Poly(*N*-acetylaniline) (PAANI) is a substituted polyaniline conducting polymer, which has been previously investigated in the fields of biosensor fabrication by our group [27–29]. Recently, we have successfully prepared a Pt nanocluster embedded with a three-dimensional (3D) matrix of PAANI nanorods on the electrode surface [30]. This composite modified glassy carbon electrode (nc-Pt/nr-PAANI/GCE) shows significantly enhanced electrocatalytic activity towards methanol oxidation. The strategy of depositing nanoparticles on to a matrix of an organic conducting polymer may find wide application in electrocatalysis. In this work we report a novel nanocomposite matrix of palladium nanoclusters deposited on to poly (*N*-acetylaniline) nanorods. The nanocomposite modified electrode has strong electrocatalytic activity towards the 4-e^- reduction of oxygen.

C. Jiang · X. Lin (✉)
Department of Chemistry, University of Science and Technology of China, Hefei 230026, China
e-mail: xqlin@ustc.edu.cn

C. Jiang
Department of Chemistry, Fudan University, Shanghai 200433, China

2 Experimental

2.1 Reagents and instruments

N-acetylaniline was purchased from the Changping-Kuangying Chemical Reagent of Beijing (Beijing, China) and used after recrystallization from ethanol. Highly pure oxygen was obtained from the Nanjing-Shangyuan Industrial Gas Company (Nanjing, China). $PdCl_2$, H_2O_2, H_2SO_4 and $HClO_4$ were obtained from the Chemical Reagent Company of Shanghai (Shanghai, China). These chemicals were analytical grade and used as received without further purification. H_2O_2 solution was freshly prepared before each experiment. Doubly distilled water was used.

Electrochemical experiments were conducted using a CHI832 electrochemistry workstation (Chen-Hua, Shanghai, China) with a three-electrode system consisting of a test electrode, a platinum wire auxiliary electrode and a saturated calomel reference electrode (SCE). A glassy carbon electrode (GCE, Φ 4.0 mm) (Lan-Like HCET Company, Tianjin, China) was used as the basal electrode for fabrication. All potentials are reported versus SCE. O_2 gas was bubbled directly into the solution for 30 min to obtain O_2-saturated solutions and was flushed over the solution during measurements. If necessary, the electrolyte solution was deoxygenated by bubbling N_2 gas for 30 min to obtain a N_2-saturated solution. Experiments were carried out at room temperature (20 ± 1 °C). Under these experimental conditions, the concentration of the dissolved oxygen in 0.5 M H_2SO_4 solution is 1.1×10^{-6} M, according to the literature [31, 32].

X-ray photoelectron spectroscopy (XPS) measurements were carried out using an ESCALAB MK2 photoelectron spectrometer (VG, UK) equipped with MgK-Alpha X-ray radiation as the excitation source, with the pressure in the chamber below 10^{-9} Torr.

X-ray diffraction patterns (XRD) were recorded on a MXPAHF rotating anode X-ray diffractometer (Japan) with Cu radiation source ($\lambda = 1.54056$ Å).

Field emission scanning electron microscopy (FE-SEM) images were obtained on a Sirion-200 instrument (FEI, Japan).

2.2 Electrode preparation

The basal GCE was first polished to a mirror finish using sand paper. After thorough cleaning, the GCE was dipped in 1.0 M $HClO_4$ solution + 0.1 M *N*-acetylaniline and subjected to cyclic voltammetry (CV) scanning between −0.2 and 1.0 V for 15 cycles at 50 mV s^{-1} for electropolymerization of *N*-acetylaniline [30]. The electrode obtained was labeled PAANI/GCE.

The PAANI/GCE was immersed in 0.5 M H_2SO_4 + 2.0 mM $PdCl_2$ solution, and was subjected to several voltage cycles between −0.3 and 0.5 V at 50 mV s^{-1}, during which the palladium nanoparticles were electrodeposited on to the polymer matrix. The electrode prepared in this way was labeled Pd/PAANI/GCE.

3 Results and discussion

3.1 Electrochemical deposition of Pd and PAANI

Figure1a shows the cyclic voltammograms (CVs) for the electrodeposition of palladium nanoparticles on PAANI/GCE. A pair of redox peaks appeared at E_m ($E_m = E_{pa}/2 + E_{pc}/2$) of 0.13 V (couple I), attributable to the redox reactions of PAANI. Another pair of small but well-developed peaks appeared at $E_m = -0.22$ V (couple II). Since the PAANI film was in a non-conducting state in the potential range from −0.3 to −0.1 V, couple II may be attributed to the reversible adsorption/desorption reaction

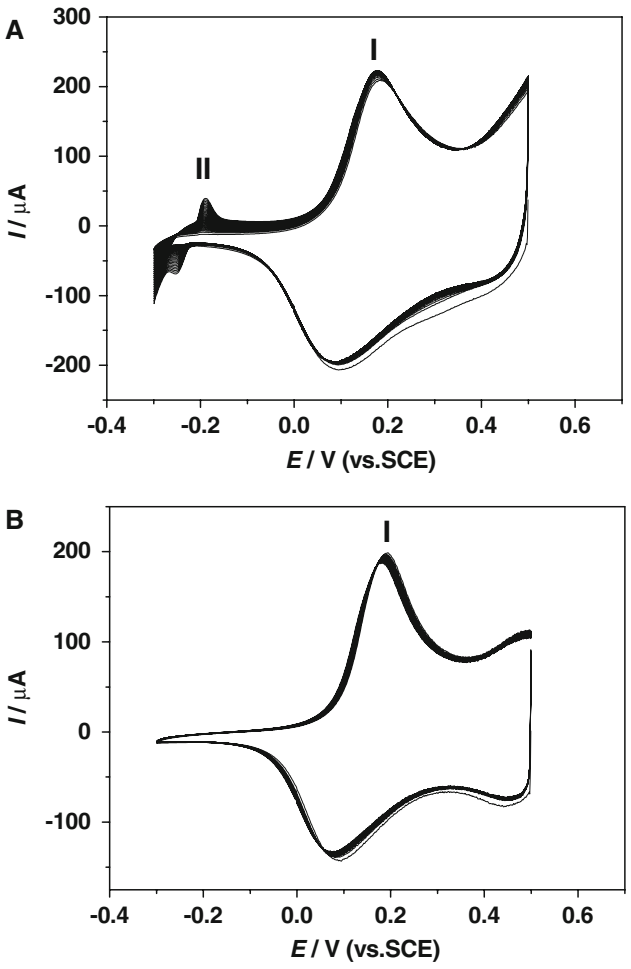

Fig. 1 Multi-cycle CVs of the PAANI/GCE (**a**) in the presence of and (**b**) in the absence of 2.0 mM $PdCl_2$ in 0.5 M H_2SO_4 solution. Scan rate: 50 mV s^{-1}

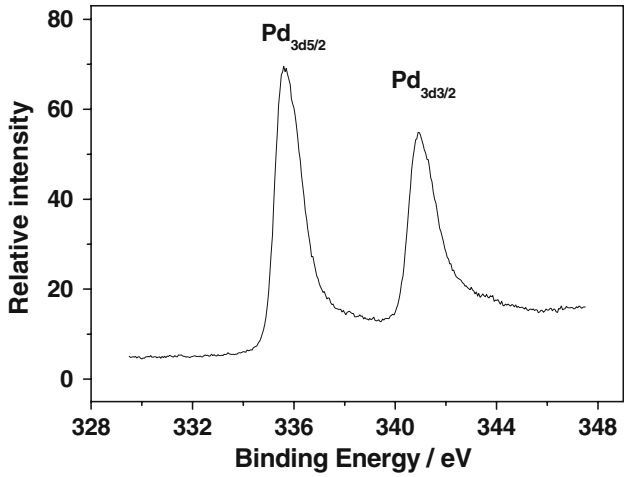

Fig. 2 The XPS of Pd/PAANI/GCE

of hydrogen on the deposited Pd nanoparticles. Certainly, the peak currents of couple II increased with increasing cycle number.

3.2 Electrode characterization

An XPS spectrum of the Pd/PAANI/GCE was obtained and is shown in Fig. 2. The two characteristic peaks of Pd $3d_{5/2}$ and Pd $3d_{3/2}$ appeared at 335.7 and 340.8 eV, respectively, indicating the presence of the Pd (0) state [33].

FE-SEM images of the electrode surface layers on the electrodes were obtained, as shown in Fig. 3. In Fig. 3a, the electrodeposited PAANI shows a nano-porous matrix consisting of a stack of nanorods. The nanorods formed are 100–200 nm in diameter and about 1 μm in length. The vertical holes in the matrix are 300–500 nm average diameter. After deposition of Pd nanoparticles on the PAANI matrix, Fig. 3b shows ball-shaped Pd nanoparticles of 50–500 nm diameter in the PAANI matrix. Some of the ball-shaped Pd nanoparticles have grown on the ends of nanorods, forming a novel nano-ball and nano-rod network, as shown in Fig. 3c. This case is quite different from that found with a previously prepared nc-Pt/nr-PAANI composite, in which the metal clusters grew so that they were embedded in the nanorods [30]. Obviously, Pd^{2+} cations had not been extracted from the solution into the PAANI nano-rod before the electrodeposition because the positively charged PAANI nano-rod can repel cations, preventing their approach. The preferred deposition on the ends of the nanorods may indicate a higher electronic conductivity along the nano-rod axis. The spherical Pd particles are expected to be clusters of much finer nanoparticles, since the Pd crystals have a face-centered cubic lattice.

To demonstrate the cluster structure, XRD patterns of the Pd/PAANI composite were obtained as shown in Fig. 3d. All XRD peaks can be indexed based on the JCPDS file [34]. Three major peaks at 40.1°, 46.4° and 67.9° can be assigned to diffraction from the (1 1 1), (2 0 0) and (2 2 0) planes, respectively, of the face-centered cubic lattice of Pd (0). The Pd particle size was calculated from the Scherrer equation [35], $\beta = \kappa\lambda/D\cos\theta$, where λ is the X-ray wavelength, κ is the shape factor (0.89), β is the average diameter of the particles, θ is the Bragg angle in degrees, and D the full-width at half-maximum of the respective diffraction peak. An average diameter was

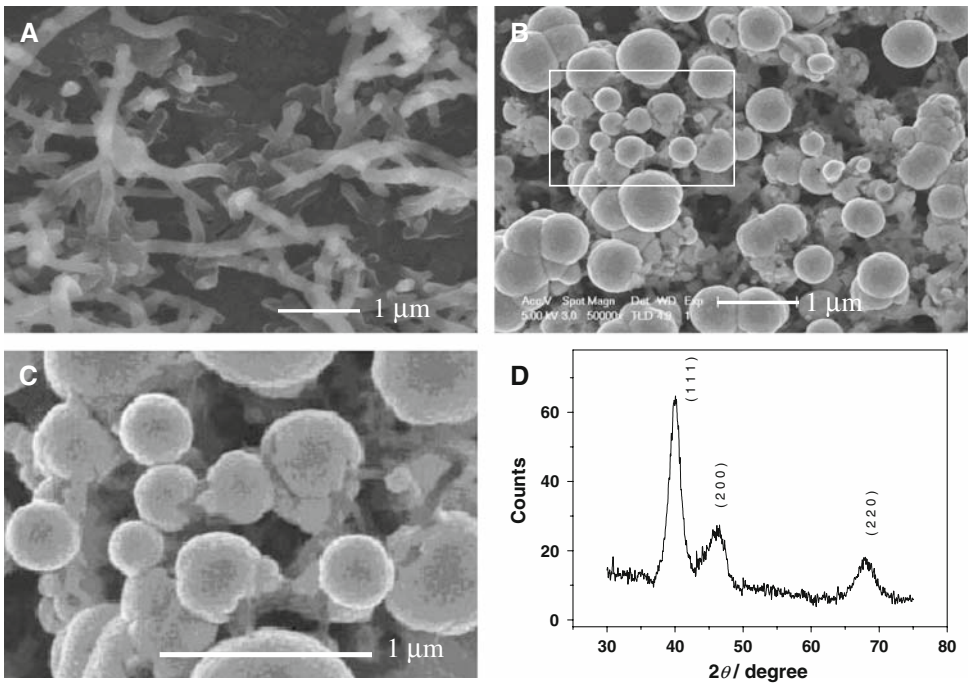

Fig. 3 FE-SEM image of (**a**) PAANI/GCE, (**b**) Pd/PAANI/GCE, (**c**) the enlarged part of (**b**). (**d**) XRD patterns of the Pd/PAANI composite

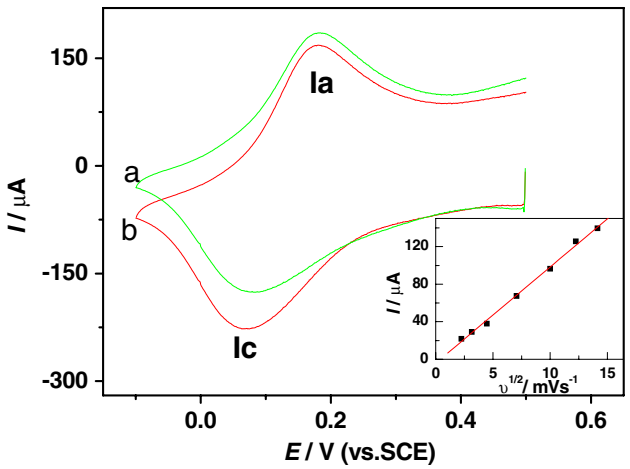

Fig. 4 CVs of the Pd/PAANI/GCE in 0.5 M H_2SO_4 solution saturated with (**a**) N_2 and (**b**) O_2. Scan rate: 50 mV s^{-1}. Inset: plot of i_{pc} versus the square root of the scan rate

calculated as 9.5 nm for the Pd crystallites. Hence, it can be concluded that the Pd nanoparticle deposits of 50–500 nm in diameter were clusters constructed from nano-Pd crystallites of 9.5 nm average size. This result is similar to that found for electrodeposited Pt nanoclusters [15, 36, 37].

3.3 Catalytic reduction of oxygen

The CV of oxygen reduction at Pd/PAANI/GCE is shown in Fig. 4. In the presence of O_2-saturated 0.5 M H_2SO_4 solution, the reduction peak current I_{pc}(I) increased (curve a) by comparison with the background current (curve b), and the peak potential shifted slightly in the negative direction. This indicates that Pd/PAANI/GCE has catalytic ability towards the ORR, which is mediated by the reduction reaction of couple (I).

The ORR in aqueous solution generally proceeds through two possible pathways [38]. One is the four-electron pathway through which molecular oxygen is directly reduced to H_2O. The other is the peroxide pathway through which molecular oxygen is first reduced to H_2O_2, followed by further reduction to H_2O. To determine the number of electrons transferred (n) during the catalytic reduction, a scan rate dependence experiment was carried out. By increasing the scan rate, the E_{pc} was shifted negatively, however, the half-peak potentials ($E_{pc/2}$) was maintained at 77 ± 8 mV. The ORR peak current i_{pc}, the difference of reduction current of the couple in 0.5 M H_2SO_4 solution saturated with N_2 or O_2, was a linear function of the square root of the scan rate ($v^{1/2}$) in the range 5–200 mV s^{-1} with a value $-4.01 \times 10^{-5} + 3.24 \times 10^{-4}$ $[v$—V s^{-1}—$]^{1/2}$ ($R = 0.9986$), as shown in Fig. 4 (inset). This relationship indicates a diffusion-controlled process with no significant adsorption accumulation. Taking the slope of this function and $C_0^*(O_2) = 1.1 \times 10^{-6}$ M and $D_0 = 1.4 \times 10^{-5}$ cm^2 s^{-1} [31, 32], n was evaluated as 4.16, based on the equation $i_p = (2.99 \times 10^{-5})n(\alpha n_a)^{1/2}AD_0^{1/2}v^{1/2}C_0^*$; $\alpha n_a = 0.37$ was evaluated from the shift of peak potential following a 10-fold increase in the scan rate. Thus the ORR on the Pd/PAANI/GCE was demonstrated to be a 1-step 4-electron reduction process.

Although the application of conducting polymers for ORR has recently been reported [39, 40], no investigation of the behavior of PAANI has been carried out. To differentiate the catalytic activity of PAANI and Pd/PAANI, chromoamperometry was used, with the results shown in Fig. 5. The current density (i), which is defined as the ratio of the peak current (I) divided by the formal electrode surface area, 0.126 cm^2, increases slowly with O_2 purging to a steady state value (~0.032 mA cm^{-2}) after about 200 s at the PAANI/GCE. By comparison, it takes only 10 s to reach the steady state (~0.635 mA cm^{-2}) at Pd/PAANI/GCE. The current density of the latter is larger than

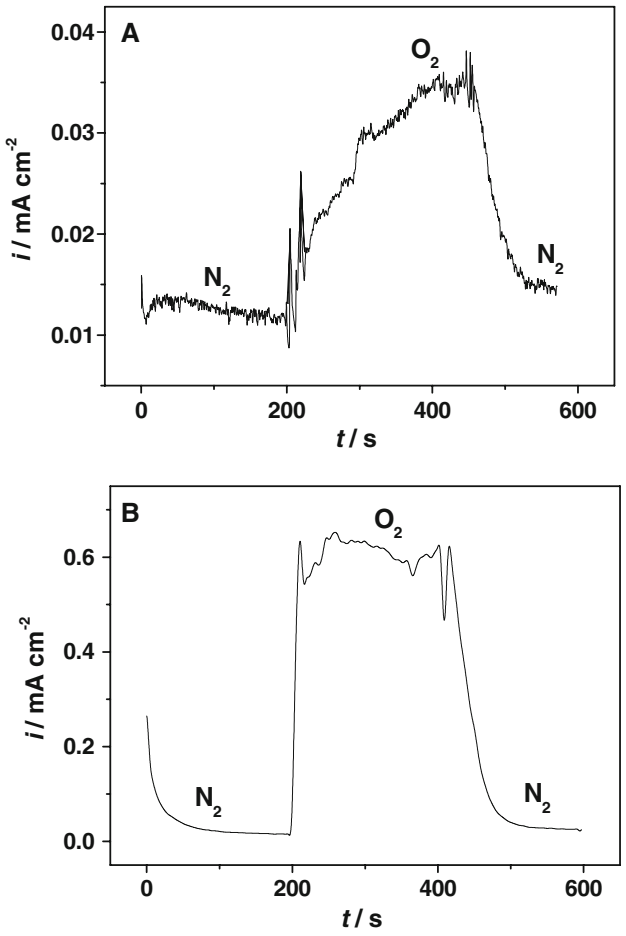

Fig. 5 Amperometric detection of O_2 reduction at 0.07 V on (**a**) the PAANI/GCE and (**b**) Pd/PAANI/GCE in 0.5 M H_2SO_4 solution purged with N_2 and O_2 alternately. A = 0.126 cm^2

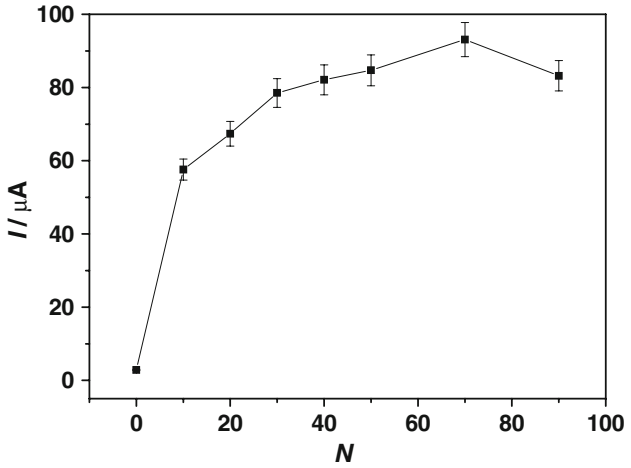

Fig. 6 The effect of cycle number (N) of the Pd electrodeposition on the oxygen reduction current. The other experimental conditions are the same as Fig. 1

that reported for the Pt-modified multiwalled carbon nanotube electrode [18]. The enhanced catalytic activity can be attributed to the existence of the Pd nanoclusters. We compared the behavior of Pd/GCE and Pd/PAANI/GCE similarly prepared and found that the Pd/GCE had lower catalytic activity toward ORR since it gave an ORR peak at 0.02, 50 mV less positive than that for Pd/PAANI/GCE at 0.07 V. Thus, the synergistic effect between Pd and PAANI is significant for both the reduction of overpotentials and the increase in ORR current density.

The effect of the cycle number (N) on the Pd electrodeposition was investigated. By altering N, the amount of deposition and the size of the deposited Pd nanoclusters can be controlled, and thus the catalytic activity can be altered. The catalytic reduction current of ORR was plotted against cycle number as shown in Fig. 6. The catalytic current increases significantly as N increases from 0 to 10, but slows down from 40 to 70, and finally tends to decrease for $N > 70$. The optimum value of $N = 70$ was selected.

Finally, the stability of Pd/PAANI/GCE was examined as an oxygen cathode at 0.07 V in 0.5 M H_2SO_4 solution. An 8% loss in the reduction current was observed after 2 h continuous electrolysis (during the test, O_2 was bubbled into the solution), which is approximately the same as for the palladium-modified carbon nanotube electrode [17].

4 Conclusions

A novel nanocomposite of Pd nanoclusters/PAANI nanorods was prepared on an electrode surface by two electrodeposition steps. The composite modified electrode (Pd/PAANI/GCE) has higher electrocatalytic activity towards the oxygen reduction reaction than the Pt-modified multiwalled carbon nanotube electrode [18]. The mechanism of oxygen reduction at the Pd/PAANI/GCE was demonstrated as a 1-step 4-electron process. The stability of the electrode suggests that there are potential applications in the development of high-efficiency fuel cells.

Acknowledgements We gratefully acknowledge financial support from the National Natural Science Foundation of China (No. 20575062).

References

1. EI-Deab MS, Ohsaka T (2002) Electrochem Commun 4:288
2. Komai YJ (1998) Exp Biol 201:2359
3. Wu S, Zhao HT, Ju HX, Shi CG, Zhao JW (2006) Electrochem Commun 8:1197
4. Osborne PG, Li XF, Li YZ, Han HW (2001) J Neurosci Res 63:224
5. Osborne PG (1997) Physiol Behav 61:485
6. Wu LN, Zhang XJ, Ju HX (2007) Biosens Bioelectron 23:479
7. Ju HX, Sheng CZ (2001) Electroanalysis 13:789
8. EI-Deab MS, Ohsaka T (2002) Electrochim Acta 47:4255
9. Zhang YR, Asahina SS, Yoshihara S, Shirakashi T (2003) Electrochim Acta 48:741
10. EI-Deab MS, Sotomura T, Ohsaka T (2005) Electrochem Commun 7:29
11. EI-Deab MS, Ohsaka T (2003) J Electroanal Chem 553:107
12. Xu WL, Zhou XC, Liu CP, Xing W, Lu TH (2007) Electrochem Commun 9:1002
13. Huang QH, Yang H, Tang YW, Lu TH, Daniel LA (2006) Electrochem Commun 8:1220
14. Tang H, Chen JH, Huang ZP, Wang DZ, Ren ZF, Nie LH, Kuang YF, Yao SZ (2004) Carbon 42:191
15. Xu YH, Lin XQ (2007) Electrochim Acta 52:5140
16. Kongkanand A, Kuwabata S, Girishkumar G, Kamat P (2006) Langmuir 22:2392
17. Lin YH, Cui XL, Ye XR (2005) Electrochem Commun 7:267
18. Cui HF, Ye JS, Zhang WD, Wang J, Sheu FS (2005) J Electroanal Chem 557:295
19. Bose CSC, Rajeshwar K (1992) J Electroanal Chem 333:235
20. Vork FTA, Barendrecht E (1990) Electrochim Acta 35:135
21. Chen CC, Bose CSC, Rajeshwar K (1993) J Electroanal Chem 350:161
22. Lai EKW, Beattie PD, Orfino FP, Simon E, Holdcroft S (1999) Electrochim Acta 44:2559
23. Yang S et al (2007) J Power Sources. 10.1016/j.jpowsour.2007.09.080
24. Swathirajan S, Mikhail YM (1992) J Electrochem Soc 139:2105
25. Cai LT, Chen HY (1998) J Appl Electrochem 28:161
26. Gao GY, Guo DJ, Li HL (2006) J Power Sources 162:1094
27. Zheng LZ, Wu SG, Lin XQ, Nie L, Rui L (2001) Analyst 126:736
28. Wu SG, Zheng LZ, Rui L, Lin XQ (2001) Electroanalysis 13:967
29. Zheng LZ, Wu SG, Lin XQ, Nie L, Rui L (2002) Macromolecules 35:6174
30. Jiang CM, Lin XQ (2007) J Power Sources 164:49
31. Couteanceau C, Crouigneau P, Leger J-M, Lamy C (1994) J Electroanal Chem 379:389
32. Salvador-Pascual JJ, Cital'an-Cigarroa S, Solorza-Feria O (2007) J Power Sources 172:229
33. Moulder JF, Stickle WF, Sobol PE, Bomben KD, Chastain J (1992) Handbook of X-ray photoelectron spectroscopy. Perkin-Elmer Corporation, Eden Prairie, USA

34. Joint Committee on Powder Diffraction Standards (1991) Diffraction data file: JCPDS International Center for Diffraction Data, Swarthmore, PA
35. Radmilovic V, Gasteiger HA, Ross PN (1995) J Catal 154:98
36. Wang SQ, Lu LP, Lin XQ (2004) Electroanalysis 16:1734
37. Lin XQ, Li YX (2006) Biosens Bioelectron 22:253
38. Yeager E (1986) J Mol Catal 38:5
39. Khomenko VG, Barsukov VZ, Katashinskii AS (2005) Electrochim Acta 50:1675
40. Barsukov VZ, Khomenko VG, Katashinskill AS, Motronyuk TI (2004) Russ J Electrochem 40:1170